Balanced Inhibition and Excitation Drive Spike Activity in Spinal Half-Centers

Rune W. Berg,[1] Aidas Alaburda,[2] Jørn Hounsgaard[1]*

Many limb movements are composed of alternating flexions and extensions. However, the underlying spinal network mechanisms remain poorly defined. Here, we show that the intensity of synaptic excitation and inhibition in limb motoneurons varies in phase rather than out of phase during rhythmic scratchlike network activity in the turtle. Inhibition and excitation peak with the total neuron conductance during the depolarizing waves of scratch episodes. Furthermore, spike activity is driven by depolarizing synaptic transients rather than pacemaker properties. These findings show that balanced excitation and inhibition and irregular firing are fundamental motifs in certain spinal network functions.

The prevailing half-center model for rhythm-generating motor circuits in the spinal cord proposes that excitatory interneurons in each half-center drive agonist motoneurons and interneurons, which in turn inhibit motoneurons and interneurons in the antagonist half-center (*1*–*5*). This reciprocal arrangement predicts half-center neurons to be excited and inhibited in alternation during rhythmic network activity. Temporally segregated excitation and inhibition would permit spinal motor networks to operate at low intensity of synaptic activity (fig. S1). Low conductance would facilitate the contribution of the intrinsic response properties of postsynaptic neurons to cell and network dynamics (*6*–*9*). We tested these predictions directly by intracellular recordings from motoneurons during scratchlike network activity in an isolated carapace–spinal cord preparation from adult turtles.

Stereotypical episodes of scratchlike network activity can be evoked by mechanical sensory stimulation in the isolated carapace–spinal cord preparation from adult turtles (*10*–*12*). To probe the neuronal organization of functional network activity, we first examined the origin of the periodic high-conductance state reported in motoneurons during scratch episodes (*12*). The periodic nerve activity recorded in parallel from the ipsilateral hip flexor nerve (Fig. 1A) served

[1]Department of Neuroscience and Pharmacology, Panum Institute, University of Copenhagen DK 2200 Copenhagen N, Denmark. [2]Department of Biochemistry and Biophysics, Faculty of Natural Sciences, Vilnius University, Ciurlionio 21/27, 03101 Vilnius, Lithuania.

*To whom correspondence should be addressed. E-mail: j.hounsgaard@mfi.ku.dk

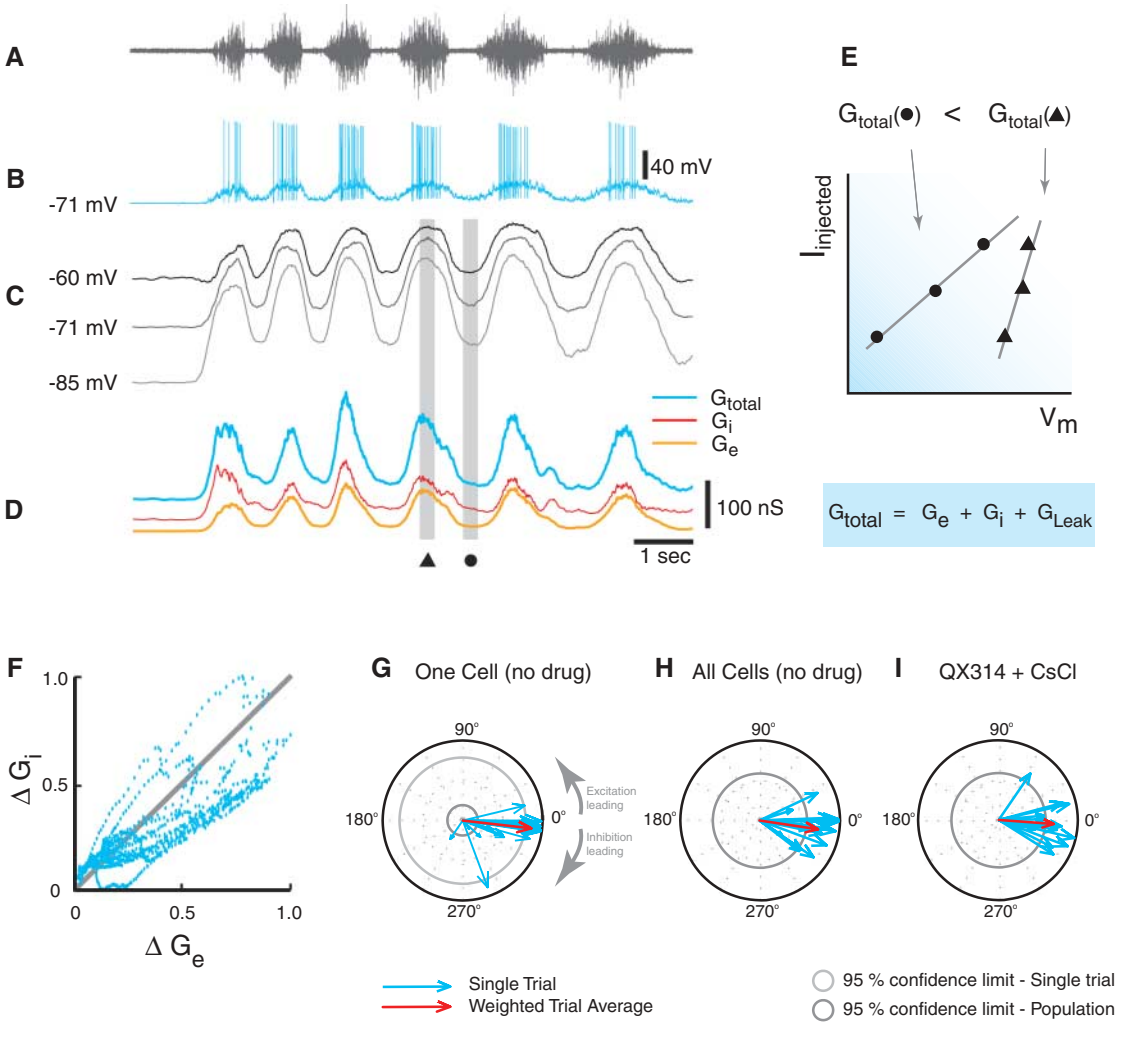

Fig. 1. Inhibition and excitation covary in motoneurons during scratching. (**A**) Hip flexor nerve activity and (**B**) intracellular recording from a motoneuron during scratch episode. (**C**) The smoothed traces of three consecutive trials at three different levels of constant holding current (from top: +1.0, 0.0, and −1.0 nA). (**D**) The mean total conductance (G_{total}) in blue was estimated from the records in (C) as the slope of the current-voltage plot at different times, as illustrated in (**E**). G_i and G_e were extracted from the equation (blue box) and from Ohm's law (*13*), as shown in (E) for the two time points marked in (D) with a circle and a triangle, respectively. (**F**) Relation between normalized increase in inhibitory and excitatory conductance (ΔG_e and ΔG_i) during scratch episodes in (D). (**G** to **I**) Population data of coherence between inhibition and excitation. Blue arrows represent single trials, and red arrows the trial average, for a single cell (G), weighted average for all cells (H), and weighted average for cells in which voltage-sensitive conductances were reduced by QX314 and Cs^+ in recording electrodes (I).

as reference for optimal temporal alignment of scratch episodes (*13*). The membrane potential V_m was recorded intracellularly from motoneurons (Fig. 1B) at different levels of holding current during successive scratch episodes (shown smoothed in Fig. 1C). With the simplifying assumptions proposed by Borg-Graham *et al.* (*14*), the average total conductance (G_{total}) and the underlying average excitatory and inhibitory conductances (G_e and G_i) were estimated from smoothened, aligned records as illustrated in Fig. 1E [see (*13*–*16*)]. In the cell illustrated and in all cells examined ($n = 16$), not only G_{total} but also G_e and G_i peaked with each depolarizing wave during scratch episodes (Fig. 1, C and D). The increases in normalized inhibitory and excitatory conductances were closely correlated ($R = 0.86$, $P << 0.05$) (Fig. 1F). Polar plots of the vectorial expression of the coherence between G_e and G_i during cyclic depolarizations clustered near a 0° phase lag for successive episodes (Fig. 1G for the cell in Fig. 1, A to D, and Fig. 1H for all 157 episodes in 16 cells). Nonsynaptic K^+ conductance recruited during depolarizing waves would contribute to the increased G_i (*16*, *17*). This was not a major factor, however, because high-conductance states and the coherence between G_e and G_i remained in 13 additional motoneurons in which spiking was eliminated and K^+ conductance was reduced by using recording electrodes containing QX314 and CsCl (Fig. 1I and fig. S2). The remaining explanation is that there is strong inhibitory synaptic activity during the depolarizing phase of the scratch.

To investigate this possibility, local inhibition was reduced pharmacologically (Fig. 2). Both amplitude and duration of the depolarizing waves increased when inhibitory synaptic input to the recorded motoneuron was reduced by addition of the glycine receptor blocker strychnine (0.1 mM) to the superfusate (Fig. 2) ($n = 5$). This shows that the depolarizing waves during scratching are limited by ongoing synaptic inhibition.

Balanced increase in excitation and inhibition perturbs the regular firing mediated by intrinsic response properties (*18*, *19*). We therefore investigated the relative role of synaptic and intrinsic conductances on the firing pattern during depolarizing waves of scratching. First, the regular firing in motoneurons, induced by a steady depolarizing current in the absence of network activity (purple in Fig. 3A), is largely determined by the intrinsic response properties. Successive action potentials (APs) are connected by the smooth voltage trajectory produced by spike after-hyperpolarizations (*20*). In contrast, firing is highly irregular during the depolarizing waves of scratch episodes (Fig. 3A, blue trace; coefficient of variation range, 0.43 to 1.2, $n = 6$), and the membrane potential undergoes rapid fluctuations between spikes (blue trace in Fig. 3A; see also Fig. 4 and fig. S3). Spike-triggered averaging revealed that APs during irregular firing are preceded by a brief depolarizing transient arising from a flat average voltage trajectory (Fig. 3B, blue; $n = 7$; see also fig. S3) in contrast to the smoothly depolarizing pacemaker potential during regular firing (purple). Thus, irregular firing is induced by depolarizing synaptic transients in the high-conductance state during network activity. A possible source of these transients is a high incidence of uncorrelated excitatory and inhibitory synaptic events (*19*, *21*). We tested the sensitivity of irregular firing during scratch episodes to successive reductions in synaptic inhibition and synaptic excitation (Fig. 3, C to E). During scratch in control conditions (Fig. 3C), irregular firing (left and middle) was revealed by the lack of correlation between the nth interspike interval (ISI) plotted against the $(n + 1)$th ISI (right) ($R < 0.2$, $n = 6$) (*22*). Reduced local inhibition (0.1 mM strychnine) rendered firing less irregular (Fig. 3D). Finally, regular firing with highly correlated ISIs was induced by a combined local reduction of inhibition and excitation (0.1 mM strychnine and 25 μM 6-cyano-7-nitroquinoxaline-2,3-dione) (Fig. 3E, bottom) [spiking during the low-amplitude depolarizing waves aided by 1.0 nA depolarizing holding current ($R = 0.56$, $p << 0.05$)]. These conditions also reduced the amplitude of the rapid synaptic fluctuations in membrane potential to a minimum. We assume that the remaining low-amplitude depolarizing waves reflect the attenuated synaptic projections from network neurons located far enough below the cut surface to be unaffected by the receptor antagonists.

Our conclusion, that motoneurons are driven by a balanced increase in excitatory and inhibitory synaptic activity, is supported by previous theoretical and experimental findings in other systems. The balanced state hampers regular firing by increasing conductance and promotes irregular firing by increasing fluctuations in membrane potential (*21*, *23*–*25*). In turtle motoneurons, regular firing driven by intrinsic response properties is severely obstructed by a conductance increase of the magnitude observed during the depolarizing waves of scratch episodes (*12*). At the same time, however, the 2- to 5-fold increase in conductance that brings the membrane potential near threshold for action potentials is associated with a parallel increase in the amplitude and frequency of voltage fluctuations and a more than 20-fold increase in integrated power spectrum in the 25- 80-Hz band (Fig. 4) (*26*). The broad spectral content associated with the rhythmic activity is fully in line with predictions for a state of intense and balanced inhibitory and excitatory synaptic activity (*16*, *19*, *21*, *24*) and orders of magnitude higher than expected for channel noise (*27*). The parallel increase in conductance and fluctuations in membrane potential during depolarizing waves, observed in all experiments analyzed ($n = 5$), is incompatible with high-conductance states mediated by a slow intrinsic conductance change.

The spinal network studied here shares several properties with the balanced state in mathematical models of large-scale random networks of inhibitory and excitatory neurons (*28*, *29*). Although the overall motor nerve activity showed little variation in successive scratch episodes, the pattern of impulse activity in individual motoneurons did (fig. S5) ($n = 10$). The raster plots of the spikes generated in a motoneuron during seven consecutive trials showed no relation between number and timing of APs during depolarizing waves within the same trial or between successive trials (Fano factor ~ 1) (see fig. S5). This suggests that the scratch network in the spinal cord produces stereotypical mo-

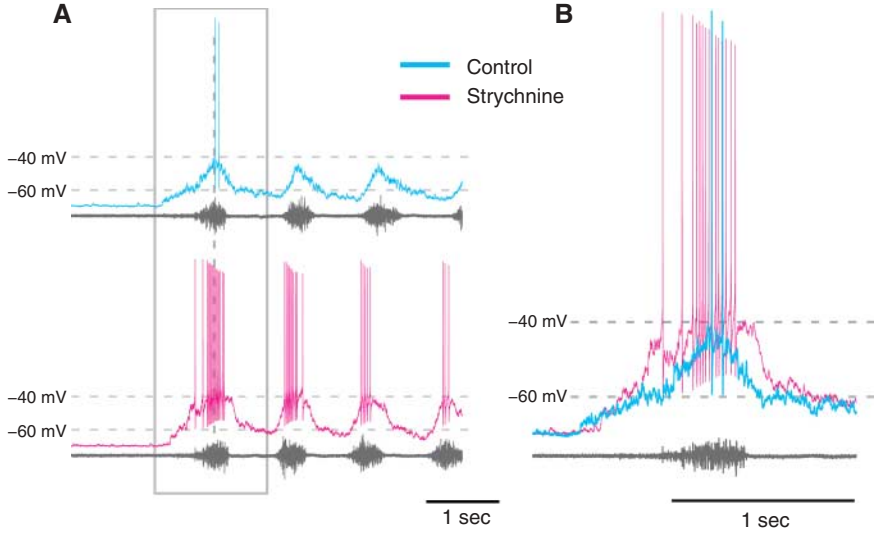

Fig. 2. Depolarizing waves enhanced by local reduction in inhibition. (**A**) Depolarizing waves in motoneuron (blue) enhanced by reduced inhibition during superfusion with strychnine (red). (**B**) Single wave highlighted.

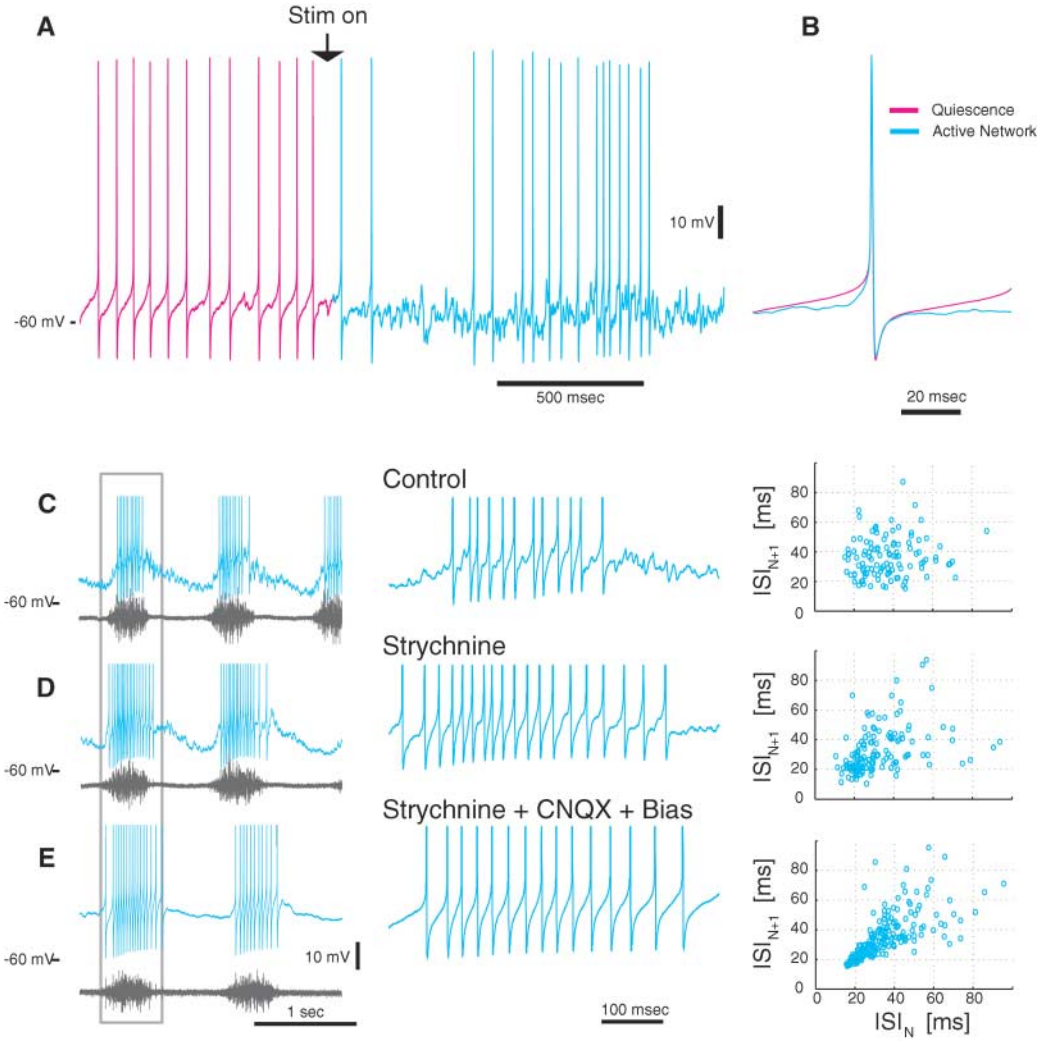

Fig. 3. Regular firing by intrinsic properties at rest, irregular firing by synaptic transients during network activity. **(A)** Regular firing in motoneuron at rest (purple) replaced by irregular firing during network activity (blue) induced at the onset of mechanical stimulus (vertical arrow). (**B**) Spikes triggered by pacemaker potential at rest and by depolarizing transient during network activity. Spike triggered averaged spikes with ~50 ms ISIs at rest (n = 50, purple) and during network activity (n = 30, blue). (**C** to **E**) Increasingly regular firing (left) and correlated ISIs (right) during scratch in control (C), reduced inhibition (D), and reduced inhibition and excitation (E). Aligned recordings from hip flexor nerve (black) and motoneuron (blue) during scratch episodes (left). Highlighted depolarizing wave (middle). Relation between successive ISIs [(n + 1)th versus nth ISI] during depolarizing waves (right).

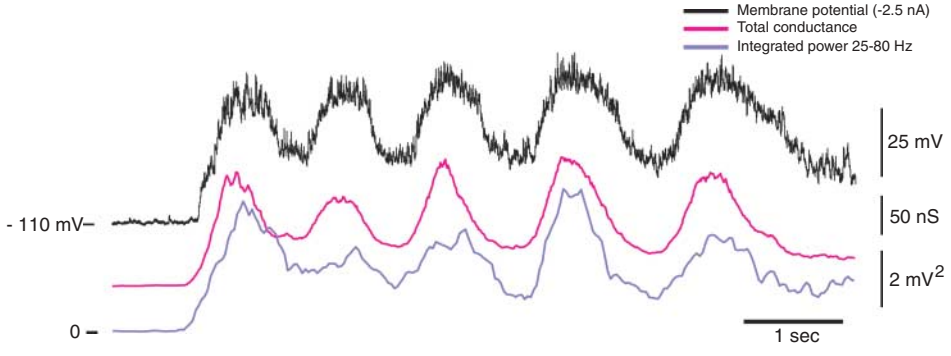

Fig. 4. The intensity of synaptic fluctuations covaries with conductance and depolarizing waves during scratching. (Upper trace) Sample intracellular recording obtained with –2.5 nA holding current. (Middle trace) G_{total} obtained as in Fig. 1C. (Lower trace) The integrated 25- to 80-Hz band power spectrum of the subthreshold membrane potential.

tor episodes in a nondeterministic way without repeating the spike patterns of individual neurons. This is in agreement with the chaotic nature of the balanced state in mathematically modeled networks in which the activity of individual neurons is stochastic and highly sensitive to initial conditions (*29*). Adopting a half-center model with balanced inhibition and excitation may help us to understand the robustness of the spinal scratch generator, its sensitivity to external input, and its ability to self organize in response to transient sensory stimuli. The high-conductance state, however, sacrifices the temporal dynamics offered by models based on weakly coupled neurons with oscillatory intrinsic properties (*6*, *7*). It remains to be seen whether high-conductance states occur throughout the scratch network or only in the motoneurons and large interneurons (*12*).

Our study suggests that balanced states of inhibitory and excitatory synaptic activity did not evolve with higher brain function (*14*, *19*, *23*, *24*, *30*) but were already present with functional motor networks in the spinal cord. The straightforward functional correlate and absence of anesthetics and other drugs makes our experimental model appealing in the search for computational advantages that balanced inhibition and excitation may provide in large-scale neural networks in general.

References and Notes

1. C. Sherrington, *The Integrative Action of the Nervous System* (Cambridge Univ. Press, Cambridge, 1947).
2. T. Graham Brown, *Proc. R. Soc. London B. Biol. Sci.* **84**, 308 (1911).

3. S. Grillner, in *Handbook of Physiology, Sect. 1: The Nervous System,* vol. 2, *Motor Control*, V. B. Brooks, Ed. (American Physiological Society, Bethesda, MD, 1981), pp. 1179–1236.
4. E. Jankowska, M. G. Jukes, S. Lund, A. Lundberg, *Nature* **206**, 198 (1965).
5. P. S. Stein, *J. Comp. Physiol. A* **191**, 213 (2005).
6. E. Marder, R. L. Calabrese, *Physiol. Rev.* **76**, 687 (1996).
7. S. Grillner, *Nat. Rev. Neurosci.* **4**, 573 (2003).
8. O. Kiehn, O. Kjaerulff, M. C. Tresch, R. M. Harris-Warrick, *Brain Res. Bull.* **53**, 649 (2000).
9. R. Delgado-Lezama, J. Hounsgaard, *Prog. Brain Res.* **123**, 57 (1999).
10. J. Keifer, P. S. Stein, *Brain Res.* **266**, 148 (1983).
11. A. Alaburda, J. Hounsgaard, *J. Neurosci.* **23**, 8625 (2003).
12. A. Alaburda, R. Russo, N. MacAulay, J. Hounsgaard, *J. Neurosci.* **25**, 6316 (2005).
13. Materials and methods are available as supporting material on *Science* Online.
14. L. J. Borg-Graham, C. Monier, Y. Fregnac, *Nature* **393**, 369 (1998).
15. J. S. Anderson, M. Carandini, D. Ferster, *J. Neurophysiol.* **84**, 909 (2000).
16. Y. Shu, A. Hasenstaub, D. A. McCormick, *Nature* **423**, 288 (2003).
17. E. A. Stern, A. E. Kincaid, C. J. Wilson, *J. Neurophysiol.* **77**, 1697 (1997).
18. W. R. Softky, C. Koch, *J. Neurosci.* **13**, 334 (1993).
19. M. N. Shadlen, W. T. Newsome, *J. Neurosci.* **18**, 3870 (1998).
20. J. Hounsgaard, O. Kiehn, I. Mintz, *J. Physiol.* **398**, 575 (1988).
21. G. L. Gerstein, B. Mandelbrot, *Biophys. J.* **4**, 41 (1964).
22. W. H. Calvin, C. F. Stevens, *J. Neurophysiol.* **31**, 574 (1968).
23. A. Destexhe, M. Rudolph, D. Pare, *Nat. Rev. Neurosci.* **4**, 739 (2003).
24. F. S. Chance, L. F. Abbott, A. D. Reyes, *Neuron* **35**, 773 (2002).
25. E. Salinas, T. J. Sejnowski, *J. Neurosci.* **20**, 6193 (2000).
26. B. Haider, A. Duque, A. R. Hasenstaub, D. A. McCormick, *J. Neurosci.* **26**, 4535 (2006).
27. K. Diba, H. A. Lester, C. Koch, *J. Neurosci.* **24**, 9723 (2004).
28. C. van Vreeswijk, H. Sompolinsky, *Neur. Comput.* **10**, 1321 (1998).
29. C. van Vreeswijk, H. Sompolinsky, *Science* **274**, 1724 (1996).
30. J. Marino *et al.*, *Nat. Neurosci.* **8**, 194 (2005).

31. This study was supported by grants from the Danish Research Council and the Lundbeck Foundation (J.H.) and a NATO Reintegration Grant (A.A.). We thank J. F. Perrier for critically reading the manuscript. Thanks to D. Kleinfeld and lab members for helpful discussions (R.B.).

Supporting Online Material

www.sciencemag.org/cgi/content/full/315/5810/390/DC1
Materials and Methods
Figs. S1 to S5
References

11 September 2006; accepted 23 November 2006
10.1126/science.1134960

Wandering Minds: The Default Network and Stimulus-Independent Thought

Malia F. Mason,[1]*§ Michael I. Norton,[2] John D. Van Horn,[1]† Daniel M. Wegner,[3] Scott T. Grafton,[1]‡ C. Neil Macrae[4]

Despite evidence pointing to a ubiquitous tendency of human minds to wander, little is known about the neural operations that support this core component of human cognition. Using both thought sampling and brain imaging, the current investigation demonstrated that mind-wandering is associated with activity in a default network of cortical regions that are active when the brain is "at rest." In addition, individuals' reports of the tendency of their minds to wander were correlated with activity in this network.

What does the mind do in the absence of external demands for thought? Is it essentially blank, springing into action only when some task requires attention? Everyday experience challenges this account of mental life. In the absence of a task that requires deliberative processing, the mind generally tends to wander, flitting from one thought to the next with fluidity and ease (*1*, *2*). Given the ubiquitous nature of this phenomenon (*3*), it has been suggested that mind-wandering constitutes a psychological baseline from which people depart when attention is required elsewhere and to which they return when tasks no longer require conscious supervision (*4*, *5*). But how does the brain spontaneously produce the images, voices, thoughts, and feelings that constitute stimulus-independent thought (SIT)?

We investigated whether the default network—brain regions that remain active during rest periods in functional imaging experiments (*6*)—is implicated in mind-wandering (*7*). The default network is minimally disrupted during passive sensory processing and attenuates when people engage in tasks with high central executive demand (*8*, *9*), which matches precisely the moments when the mind is most and least likely to wander (*2*, *4*, *5*). We thus trained individuals to become proficient on tasks (*10*) so that their minds could wander when they performed practiced versus novel task sequences (*11*). Although previous research has compared brain activity during rest to that during engagement in a task (*12*), the present investigation assesses directly both the production of SIT and activity in the default network during tasks that allow for varying degrees of mind-wandering.

Despite its regular occurrence, not all minds wander to the same degree; individuals exhibit stable differences in their propensity to produce SIT (*1*, *3*). If regions of the default network underpin the mind's wandering, then the magnitude of neural activity in these regions should track with people's proclivity to generate SIT. Specifically, individuals who report frequent mind-wandering should exhibit greater recruitment of the default network when performing tasks that are associated with a high incidence of SIT.

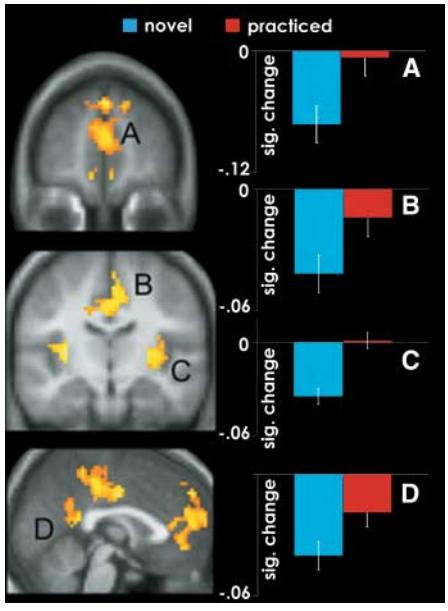

Fig. 1. Graphs depict regions of the default network exhibiting significantly greater activity during practiced blocks (red) relative to novel blocks (blue) at a threshold of $P < 0.001$, number of voxels (k) = 10. Mean activity was computed for each participant by averaging the signal in regions within 10 mm of the peak, across the duration of the entire block. Graphs depict the mean signal change across all participants. (**A**) Left (L.) mPFC (BA 9; –6, 54, 22); (**B**) Bilateral (B.) cingulate (BA 24; 0, –7, 36); (**C**) Right (R.) insula (45, –26, 4); and (**D**) L. posterior cingulate (BA 23/31; –9, –39, 27). Activity is plotted on the average high-resolution anatomical image and displayed in neurological convention (left hemisphere is depicted on the left).

[1]Department of Psychological and Brain Sciences, Dartmouth College, Hanover, NH 03755, USA. [2]Harvard Business School, Harvard University, Boston, MA 02163, USA. [3]Department of Psychology, Harvard University, Cambridge, MA 02138, USA. [4]School of Psychology, University of Aberdeen, Aberdeen AB24 2UB, Scotland.

*Present address: Martinos Center for Biomedical Imaging, MGH, Charlestown, MA 02129, USA.
†Present address: Department of Neurology, University of California, Los Angeles, CA 90095, USA.
‡Present address: Department of Psychology, University of California, Santa Barbara, CA 93106, USA.
§To whom correspondence should be addressed. E-mail: malia@nmr.mgh.harvard.edu